



Contents lists available at ScienceDirect

Chinese Chemical Letters

journal homepage: www.elsevier.com/locate/cclet

Communication

Nucleic acids induced peptide-based AIE nanoparticles for fast cell imaging

Wenjun Li^{a,b,1}, Yaping Zhang^{a,b,1}, Yanchao Wang^{c,1}, Yue Ma^{a,b}, Dongyuan Wang^a, Heng Li^d, Xiyang Ye^{e,*}, Feng Yin^{a,b,*}, Zigang Li^{a,b,*}^a State Key Laboratory of Chemical Oncogenomics, School of Chemical Biology and Biotechnology, Peking University Shenzhen Graduate School, Shenzhen 518055, China^b Pingshan Translational Medicine Center, Shenzhen Bay Laboratory, Shenzhen 518055, China^c Shenzhen Youwei Technology Holdings Group Co., Ltd., Shenzhen 518055, China^d Department of Chemistry, Tsinghua University Shenzhen International Graduate School, Shenzhen 518055, China^e Department of Gynecology, Shenzhen People's Hospital, Shenzhen 518020, China

ARTICLE INFO

Article history:

Received 25 September 2020

Accepted 28 September 2020

Available online 29 September 2020

Keywords:

Peptide-based AIE nanoparticles

Nucleic acids

Cell imaging

ABSTRACT

Herein, we utilized nucleic acids induced peptide co-assembly strategy to develop novel nucleic acids induced peptide-based AIE (NIP-AIE) nanoparticles. Strong fluorescent of AIE could be observed when a little amount of nucleic acids was added into the peptide solution, and the intensity could be regulated by the concentration of nucleic acids. This AIE nanoparticle with good biocompatibility could achieve fast cell imaging. It is also proved that the fluorescence intensity of AIE decreased with time, which indicates that the reducible cross-linkers of Wpc peptide by GSH and nanoparticles gradually disintegrate in cell. Based on the different of AIE fluorescence signals which regulated by the formation and disintegration of nanoparticles, this AIE system is expected to be used for real-time monitoring of drug release from peptide-based nano carriers *in vivo* or *in vitro*, and may provide a new platform for the construction of other organic AIE nanoparticles.

© 2020 Chinese Chemical Society and Institute of Materia Medica, Chinese Academy of Medical Sciences. Published by Elsevier B.V. All rights reserved.

Aggregation induced emission (AIE) is a unique phenomenon that overcomes aggregation-caused quenching (ACQ) effect [1–3]. The restriction of intermolecular rotations (RIR) of AIE molecules restricts the non-radiative pathway, and light up the AIE molecules [4–7]. For example, by gradually adding H₂O into the organic solution with AIE molecules, the low solubility of organic AIE molecules in water could cause the aggregation of AIE molecules and emit strong fluorescent signal [8–12]. Based on the principle of RIR, a variety of AIE molecules have been obtained by rationally designing of the core structures of AIE luminogens, including tetraphenyl ethylene (TPE) analogues [13,14], heteroatom-containing AIE molecules [15–19], intra-molecular hydrogen bond containing AIEs [20,21], and so on.

Some of the interesting features are introduced into these molecules. Just like quantum dots and carbon dots [22,23], One of the most important applications of AIE molecules is served as bio-probes for cell imaging [24–30]. Leung *et al.* designed a photo-stable AIE sensor for specific mitochondrial imaging of HeLa cells [31]. Qin *et al.* developed a series of AIE molecular analogues with far-red/near-infrared property [32]. Furthermore, many AIE derivatives were developed for the sensing of biomolecules (such as nucleic acids) [33,34]. Hong's and Wang's recent works demonstrated that cationic TPE derivatives (E)-TPEDEPy-DBz could interact with ssDNA (single-stranded DNA) by electrostatic interaction, and as a high-sensitivity probe for detection of nucleic acids [35,36].

Apart from the utilization of the solubility difference, the development of nanotechnology inspires us a novel initiation strategy for AIE fluorescence [37–39]. Nanoparticles or nanomedicine which developed through electrostatic interactions or hydrophobic interactions inducing self-assembly of biomaterials have shown obvious drug delivery advantages (lower cytotoxicity, higher permeability and tumor cell targeting) [40–43].

Recently, we developed “nucleic acids induced peptide-based co-assembly nanoparticles” as siRNA/aptamer nanocarriers for

* Corresponding authors at: State key Laboratory of Chemical Oncogenomics, School of Chemical Biology and Biotechnology, Peking University Shenzhen Graduate School, Shenzhen 518055, China.

** Corresponding author.

E-mail addresses: szyxy2009@qq.com (X. Ye), yinfeng@pkusz.edu.cn (F. Yin), lizg@pkusz.edu.cn (Z. Li).

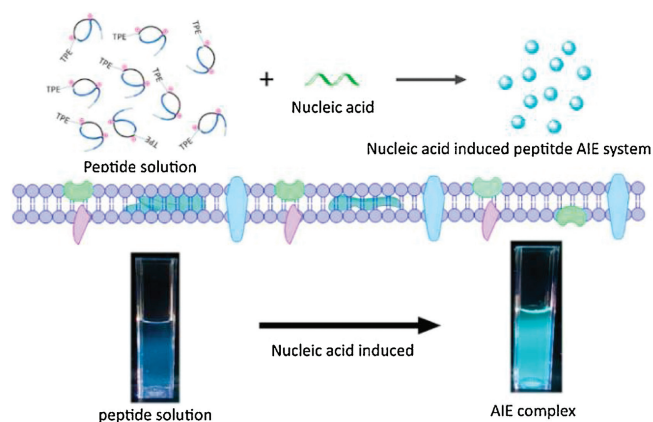
¹ These authors contribute equally to this work.

potential cancer therapy. Compared with linear peptide, the stabilized peptide with reducible cross-linkers (Fmoc-RRMEHR-MEW, with stabilized modification, as shown in Table S1 and Fig. S8 in Supporting information) showed the highest loading ability and cell membrane permeability [44–46]. The peptide Wpc could spontaneously co-aggregate with the addition of nucleic acids into uniform nanoparticles with low cytotoxicity. We envisioned that the AIE-labelled peptide Wpc may also be induced assembly by nucleic acids, activated the RIR effect and lighted up the nanoparticles. Based on this design, herein, we report the nucleic acids induced peptide-based AIE (NIP-AIE) nanoparticles with nucleic acids as regulators for cell imaging.

In this work, we synthesized the TPE labelled Wpc peptide. When a little amount of nucleic acids (RNA, primer, aptamer or plasmid) was added, a strong fluorescent of AIE could be observed, and the fluorescent intensity could be regulated by the amounts of nucleic acids. The highly normalized curve indicated that this NIP-AIE system could be potentially utilized as the AIE based nucleic acids detector. Then, AFM, SEM and DLS results further demonstrated the formation of NIP-AIE nanoparticles. Besides, the nucleic acids induced peptide AIE (NIP-AIE) nanoparticles displayed low cytotoxicity and could achieve fast cell imaging in HeLa and HEK-293 T cells. This peptide-based AIE system with nucleic acids as regulators for AIE process may provide a new platform for the construction of other organic AIE nanoparticles. We believe with appropriate choose of AIE molecules, these NIP-AIE systems could be further utilized as a novel fluorescent detection probe for nucleic acids.

Based on our design (Scheme 1), TPE-labelled Wpc peptide with reducible cross-linkers was synthesized and analyzed by LC-MS (Fig. S8). After addition of a little amount of nucleic acids (RNA) into peptide aqueous solution, significant fluorescent signals could be observed under UV irradiation (Fig. 1A). This nucleic acids induced peptide-based (NIP) AIE system displayed the similar fluorescent properties of TPE with the maximum emission wavelength at 480 nm (Fig. 1B) and fluorescent lifetime in nanoseconds (ns) level (Fig. S1B in Supporting information). As for other nucleic acids, including aptamer, plasmid, and primer could also induce and active the AIE fluorescence at the end of Wpc peptide. The excitation and emission spectrum of each kind of nucleic acid induced peptide-based AIE fluorescent were summarized in Fig. S2 (Supporting information).

Interestingly, the fluorescent intensity could be regulated by the amounts of additional nucleic acids (Figs. 1C and D, and Fig. S1A and Table S2 in Supporting information). As shown in Fig. 1C, with the gradually increased concentrations of siRNA, the fluorescent intensity of NIP-AIE at 480 nm was improved



Scheme 1. Schematic illustration of the nucleic acids induced peptide-based AIE (NIP-AIE) system.

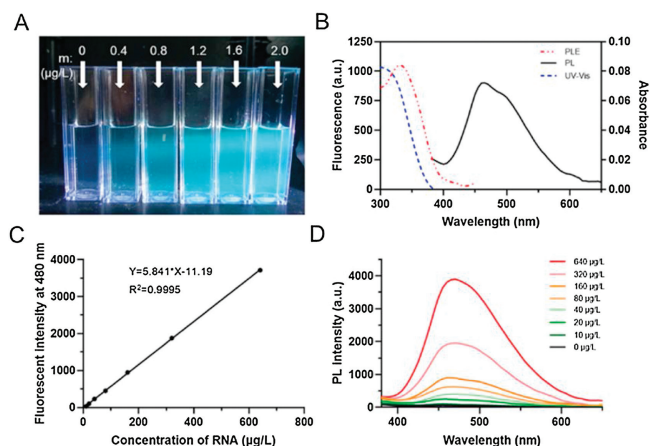


Fig. 1. Confirmation of nucleic acids (RNA) induced Strong AIE fluorescent by self-assembly of TPE-peptide. (A) Photographs of NIP-AIE nanoparticles in 2.5 mL ddH₂O. (B) PL and UV spectrum of NIP-AIE nanoparticles. (C) Standard curve of fluorescent intensity at 480 nm of (D). (D) PL spectrum of 40 μg TPE-Wpc peptide with different amounts of RNA. $E_x = 330$ nm, $E_m = 480$ nm.

correspondingly, and the curve was fitted with the linear relationship $y = ax + b$ (y is the fluorescent intensity at 480 nm (au), x is the concentrations of nucleic acids ($\mu\text{g/L}$), a and b are the corresponding parameters.). For RNA induced TPE-Wpc-based AIE system, $a = 5.841$, $b = -11.19$, $R^2 = 0.9995$. The fluorescent intensity of this NIP-AIE system could be regulated by the additional nucleic acids with the linear relationship, may demonstrated that further utilized this AIE system as a novel fluorescent detection probe for nucleic acids.

The AIE fluorescence was contributed to the co-assembly process between peptide and nucleic acids. Thus, the characterizations were further conducted to analyze the nucleic acids-peptide co-assembly AIE nanoparticles. As shown in Fig. 2, both the atomic-force microscopy (AFM) and scanning electron microscopy (SEM) showed clear formation of nanoparticles about 100 nm. Dynamic light scattering (DLS) data indicated the hydrodynamic sized of NIP-AIE nanoparticles were about 100 nm (Fig. S4A in Supporting information), which be consistent with the electron microscope data. We assume that the self-assembly of NIP-AIE nanoparticles is induced by electrostatic interaction, and the negative charged nucleic acid will inevitably lead to the potential

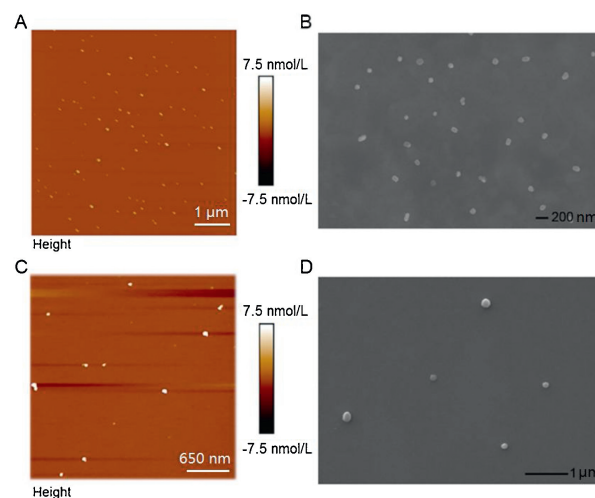


Fig. 2. AFM and SEM characterizations of nucleic acids induced peptide-based AIE nanoparticles. (A, B) Primer induced NIP-AIE nanoparticles. (C, D) RNA induced NIP-AIE nanoparticles.

decrease of Wpc with positive charge. In order to verify this hypothesis, zeta potential data of Wpc solution before and after nucleic acid addition were collected. As shown in Fig. S4B (Supporting information), the potential value of pure WPC solution is 24.8 ± 1.3 mV, and the value of NIP-AIE nanoparticles decreased to 14.0 ± 2.4 mV, which also indicated that the nanoparticles are effectively assembled.

The selectivity of nucleic induced peptide-based NIP-AIE nanoparticles were also being verified. Plasmids and poly(sodium 4-styrenesulfonate) with larger molecular weights, and anionic reagent dNTP were added to the TPE-Wpc aqueous solution separately. When the oligonucleotides were replaced by longer plasmids (~7000 bp) or poly(sodium 4-styrenesulfonate) (Mw~7000), the microstructure of the nanostructures was not fixed even though the peptide could aggregate (Figs. S3A-C in Supporting information). While, dNTP was added in peptide solution can hardly induce AIE fluorescence (Fig. S3D in Supporting information). We speculate that the main application limitation of AIE nanoparticles as nucleic acid detection signals is suitable for limited length oligonucleotides.

Before the characterization of biocompatibility and cell imaging of this peptide-based AIE system, the stability of the nanoparticles in different environments was evaluated. As shown in Fig. S5 (Supporting information), the almost immutable fluorescence intensity of NIP-AIE in PBS (pH 7.4) and ddH₂O at 37 °C was detected for more than 24h, which indicated nanoparticles were stable under near-neutral conditions. This characteristic would provide convenience for further application for biological systems.

According to the MTT assay protocol, different concentrations of NIP-AIE nanoparticles were incubated with HeLa and HEK-293 T cells, the biocompatibility of nanoparticles was evaluated by evaluating relative cell survival. As shown in Figs. 3A and B, low cytotoxicity of this NIP-AIE nanoparticles was observed in both HeLa and HEK-293 T cell lines. These results demonstrated that for both HeLa and HEK-293 T cells, the TPE-Wpc-based AIE nanoparticles displayed low cytotoxicity and high biocompatibility.

Then, the potential of this nanoparticles for cellular imaging was evaluated. In order to locate the blue fluorescence of NIP-AIE which introduced by TPE aggregation, the red nuclear fluorescent dye Reddot2 was chosen to stain the nucleus. As shown in Figs. 3C–J, strong fluorescent signals could be observed in both HeLa and HEK-293 T cells after 12 min incubation, which demonstrated that this NIP-AIE nanoparticles could achieve fast cell imaging. As the co-incubated time was prolonged to 4 h (Fig. S6 in Supporting information), obvious AIE fluorescence could still be detected in HeLa cell. Continue to extend the time to 12 h and 24 h, the blue AIE signals in cell gradually weakened. The similar phenomenon was also found in HEK-293 T cell (Fig. S7 in Supporting information). This may be due to the gradual degradation of peptide-based nanoparticles in cells, and the aggregation induced emission effect was relieved. After more data collecting, this AIE system may be used for real-time monitoring of drug release from peptide-based nano carriers *in vivo* or *in vitro*.

The phenomenon of AIE usually needs the steric hindrance of hydrophobic groups to activate the RIR effect. Based on this principle, many cell image AIE probes and DNA sensing probes have been developed. Apart from the regulation of the solubility difference of AIE molecule derivatives by chemical modification, the self-assembly nanotechnology inspires us a novel initiation idea about AIE fluorescence. In this work, we utilized nucleic acids induced peptide assembly into nanoparticles. The TPE molecule at the end of the peptide produced strong AIE fluorescence due to the aggregation of peptide. In this system, the additional nucleic acids can be served as fluorescent regulators to detect the delivery and release of cargos in cells. It is also proved that this novel peptides-based AIE nanoparticle with good biocompatibility for fast cell image and real-time monitoring the metabolic process of intracellular nanoparticles. Using AIE nanoparticles system to study the release of drugs will be promising research directions. Furthermore, the modifiable end of the peptide and some special amino acid side chain groups provide appropriate sites for the covalent attachment of other AIE molecules, and more in-depth attempt on the construction of other organic AIE nanoparticles is valuable.

Declaration of competing interest

The authors declare that they have no known competing financial interests or personal relationships that could have appeared to influence the work reported in this paper.

Acknowledgments

We acknowledge financial support from the Natural Science Foundation of China (Nos. 21778009, 21977010 and 81701818); the Natural Science Foundation of Guangdong Province (No. 2020A1515010522); the Guangdong Foundation for Basic and Applied Basic Research (No. 2019A1515110365); the Shenzhen Science and Technology Innovation Committee (Nos. JCYJ20180507181527112, JCYJ201805081522131455 and JCYJ20170817172023838); the China Postdoctoral Science Foundation (No. 2020M670054). We acknowledge financial support from Beijing National Laboratory of Molecular Science open grant (No. BNLMS20160112) and Shenzhen-Hong Kong Institute of Brain Science-Shenzhen Fundamental Research Institutions (No. 2019SHIBS0004). This work is supported by High-Performance Computing Platform of Peking University.

Appendix A. Supplementary data

Supplementary material related to this article can be found, in the online version, at doi:<https://doi.org/10.1016/j.ccl.2020.09.054>.

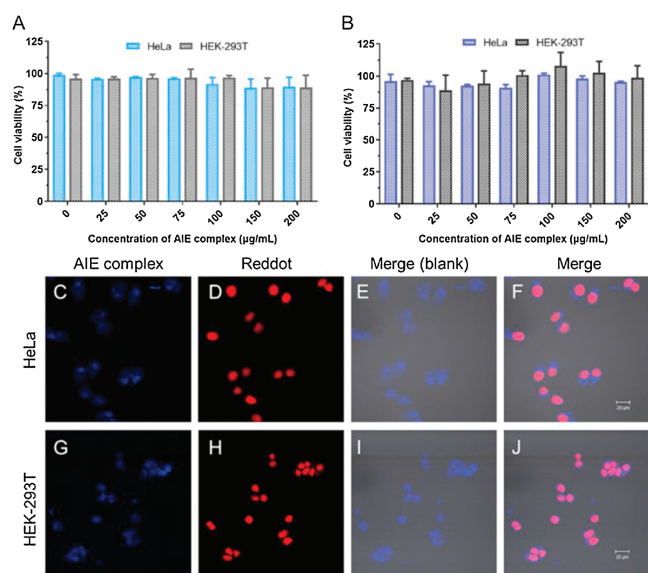


Fig. 3. AIE nanoparticle with good biocompatibility could achieve fast cell imaging. The cell viability of HeLa and HEK-293 T treated with primer (A) or RNA (B) induced NIP-AIE nanoparticles was detected by MTT cell viability assay. (C–J) Confocal microscopy imaging of HeLa and HEK-293T cells incubated with NIP-AIE nanoparticles (20 μg/mL) for 12 min. (C, G), AIE at 405 nm; (D, H): red dot at 633 nm; (E, F, I, J) merge images. Scale bar is 20 μm.

References

- [1] Y. Hong, J.W. Lam, B.Z. Tang, *Chem. Soc. Rev.* 40 (2011) 5361–5388.
- [2] X. He, Z. Zhao, L.H. Xiong, et al., *J. Am. Chem. Soc.* 140 (2018) 6904–6911.
- [3] W.Z. Yuan, H. Zhao, X.Y. Shen, et al., *Macromolecules* 42 (2009) 9400–9411.
- [4] Y. Yu, C. Feng, Y. Hong, et al., *Adv. Mater.* 23 (2011) 3298–3302.
- [5] P. Wei, J.X. Zhang, Z. Zhao, et al., *J. Am. Chem. Soc.* 140 (2018) 1966–1975.
- [6] X. Zhang, X. Zhang, L. Tao, et al., *J. Mater. Chem. B* 2 (2014) 4398–4414.
- [7] J. Wang, X. Gu, P. Zhang, et al., *J. Am. Chem. Soc.* 139 (2017) 16974–16979.
- [8] Z. Zhou, X. Yan, M.L. Saha, et al., *J. Am. Chem. Soc.* 138 (2016) 13131–13134.
- [9] J. Liu, J.W. Lam, B.Z. Tang, *Chem. Rev.* 109 (2009) 5799–5867.
- [10] F. Bu, R. Duan, Y. Xie, et al., *Angew. Chem. Int. Ed.* 127 (2015) 14700–14705.
- [11] J. Liu, Y. Zhong, J.W. Lam, et al., *Macromolecules* 43 (2010) 4921–4936.
- [12] Z. Luo, X. Yuan, Y. Yu, et al., *J. Am. Chem. Soc.* 134 (2012) 16662–16670.
- [13] Y. Hong, J.W. Lam, B.Z. Tang, *Chem. Commun.* (2009) 4332–4353.
- [14] M. Gao, Q. Hu, G. Feng, et al., *J. Mater. Chem. B* 2 (2014) 3438–3442.
- [15] Z. Ning, Z. Chen, Q. Zhang, et al., *Adv. Funct. Mater.* 17 (2007) 3799–3807.
- [16] M. Han, M. Hara, *Am. Chem. Soc.* 127 (2005) 10951–10955.
- [17] H.C. Su, O. Fadhel, C.J. Yang, et al., *J. Am. Chem. Soc.* 128 (2006) 983–995.
- [18] T. Baumgartner, R. Réau, *Chem. Rev.* 106 (2006) 4681–4727.
- [19] Y. Li, F. Li, H. Zhang, et al., *Chem. Commun.* (2007) 231–233.
- [20] T. Mutai, H. Tomoda, T. Ohkawa, et al., *Angew. Chem. Int. Ed.* 120 (2008) 9664–9666.
- [21] S. Scheiner, V.M. Kolb, *Natl. Acad. Sci. U. S. A.* 77 (1980) 5602–5605.
- [22] D. Wu, D. Wang, X. Ye, et al., *Chin. Chem. Lett.* 31 (2020) 1504–1507.
- [23] S. Sun, Q. Guan, Y. Liu, et al., *Chin. Chem. Lett.* 30 (2019) 1051–1054.
- [24] S. Kim, H.E. Pudavar, A. Bonoiu, et al., *Adv. Mater.* 19 (2007) 3791–3795.
- [25] M. Gao, B.Z. Tang, *Drug Discov. Today* 22 (2017) 1288–1294.
- [26] W. Wang, L. Zhu, Y. Hirano, et al., *Anal. Chem.* 88 (2016) 7991–7997.
- [27] X. Zhang, X. Zhang, B. Yang, et al., *RSC Adv.* 3 (2013) 9633–9636.
- [28] Q. Xia, Z. Chen, Z. Yu, et al., *ACS Appl. Mater. Inter.* 10 (2018) 17081–17088.
- [29] Y. Hong, L. Meng, S. Chen, et al., *J. Am. Chem. Soc.* 134 (2012) 1680–1689.
- [30] H. Shi, R.T. Kwok, J. Liu, et al., *J. Am. Chem. Soc.* 134 (2012) 17972–17981.
- [31] C.W.T. Leung, Y. Hong, S. Chen, et al., *J. Am. Chem. Soc.* 135 (2013) 62–65.
- [32] W. Qin, D. Ding, J. Liu, et al., *Adv. Funct. Mater.* 22 (2012) 771–779.
- [33] X. Xu, J. Li, Q. Li, et al., *Chem. Eur. J.* 18 (2012) 7278–7286.
- [34] D. Ding, K. Li, B. Liu, et al., *Accounts Chem. Res.* 46 (2013) 2441–2453.
- [35] Y. Hong, H. Xiong, J.W.Y. Lam, et al., *Chem. Eur. J.* 16 (2010) 1232–1245.
- [36] Z. Wang, Y. Gu, J. Liu, et al., *J. Mater. Chem. B* 6 (2018) 1279–1285.
- [37] Y.F. Xiao, F.F. An, J.X. Chen, et al., *Small* 15 (2019) 1903121.
- [38] Y. Sun, W. Ma, Y. Yang, et al., *Asian J. Pharm. Sci.* 14 (2019) 581–594.
- [39] Z. Chen, C. Wu, Z. Zhang, et al., *Chin. Chem. Lett.* 29 (2018) 1601–1608.
- [40] J. Nam, S. Son, K.S. Park, et al., *Nat. Rev. Mater.* 4 (2019) 398–414.
- [41] P. Zheng, Y. Liu, J. Chen, et al., *Chin. Chem. Lett.* 31 (2020) 1178–1182.
- [42] D. Li, T. Su, L. Ma, et al., *Eur. J. Med. Chem.* (2020) 112367.
- [43] J. Wang, W. Xu, S. Li, et al., *J. Biomed. Nanotechnol.* 14 (2018) 2102–2113.
- [44] W. Li, D. Wang, X. Shi, et al., *Mater. Horizons* 5 (2018) 745–752.
- [45] X. Shi, R. Zhao, Y. Jiang, et al., *Chem. Sci.* 9 (2018) 3227–3232.
- [46] Y. Ma, W. Li, Z. Zhou, et al., *Bioconjugate Chem.* 30 (2019) 536–540.